

Interfacial hydrodynamic modes at a solid-liquid interface by light scattering

E. F. Gramsbergen, A. H. Stiphout, and G. H. Wegdam

Laboratory for Physical Chemistry, Nieuwe Achtergracht 127, 1018 WS Amsterdam, The Netherlands

(Received 12 June 1989)

Using Brillouin scattering from an evanescent wave, an interfacial fluid mode has been observed at a solid-liquid interface. Its dispersion relation depends on the component of the wave vector parallel to the interface and is, within the accuracy of the experiment, linear with a speed equal to the bulk sound speed. Also observed is the Rayleigh mode at the solid side of the interface whose width is consistent with mode-coupling theory.

INTRODUCTION

Interfaces induce long-range correlations in liquids that decay exponentially from the interface into the bulk. Fluctuating hydrodynamics predicts such correlations at a liquid-solid interface, as a result of thermally excited interfacial fluid modes.^{1,2} At much lower frequency, interface modes are known that are very similar; these modes, however, are excited by some external source instead of being thermally excited.³ Brillouin scattering has been used extensively to study liquid-solid interfaces^{4,5} and surface modes in solids.^{5,6} The dispersion relation of the fluid modes near a liquid-solid interface depends on the component of the wave vector parallel to the interface, k_{\parallel} , and is, in the small- k_{\parallel} limit, linear with a speed which depends on the bulk sound speeds and densities in the two media. When either $\rho/\rho_s \ll 1$ or $c/c_i \ll 1$, where ρ and ρ_s are the liquid and solid densities and c and c_i are the liquid and transverse solid sound velocities, the velocity c_i of the fluid interface mode is equal to the bulk velocity c . For larger values of k_{\parallel} , the interfacial fluid modes are modified by additional viscous dissipation caused by the solid walls, and by the transport of heat across the interface. Mode coupling with these viscous and heat modes then results in a dispersion relation which is no longer linear.^{1,2} Our measurements, however, are in the linear regime with $c_i = c$. The new element in this work is the measurement of the dynamic structure factor $S(\mathbf{k}, \omega)$ for different values of \mathbf{k} , which enables us to verify whether the dispersion relation is linear in k_{\parallel} and independent of k_{\perp} as predicted.

EXPERIMENT

An argon-ion laser beam (wavelength $\lambda = 514$ or 488 nm) is focused onto the center of the base of a smoothly polished quartz semicylinder (see Fig. 1, inset). The semicylinder is immersed in a large bath filled with liquid. The normal on its base lies in the scattering plane. The angle of incidence of the laser beam on the quartz base ϕ is slightly below the critical angle of total reflection ϕ_c . The beam is totally reflected at the quartz-liquid interface while an evanescent wave is generated in the liquid. The field of the evanescent wave decays exponentially from

the interface into the bulk with a typical penetration depth of $1 \mu\text{m}$ for $\phi = \phi_c - 0.2^\circ$. This field, with a frequency $\omega_i/2\pi$ and a real wave vector \mathbf{k}_i parallel to the interface, acts as a source for scattering. The scattered radiation with frequency $\omega_f/2\pi$ and wave vector \mathbf{k}_f is collected, analyzed by a triple-pass Burleigh DAS-10 Fabry-Perot (FP) interferometer with a 11.2-mm spacing between the mirrors (a free spectral range $\nu_{\text{FSR}} = 2.68 \times 10^{10} \text{ s}^{-1}$), and detected by a photomultiplier in order to obtain the dynamic structure factor $S(\mathbf{k}, \omega)$, with $\omega = \omega_f - \omega_i$, for a fixed value of $\mathbf{k} = \mathbf{k}_f - \mathbf{k}_i$.⁷ The scattering vector \mathbf{k} was varied either by changing the scattering angle θ or, incidentally, by switching from the 514 nm to the less intense 488-nm line.

In measuring with \mathbf{k} not parallel to the interface, we implicitly use the fact that interface modes are localized in a region which is very small in one direction (perpendicular to the interface). This localization implies that a single mode has Fourier components which all have the same k_{\parallel} but different k_{\perp} . Their distribution is centered around $k_{\perp} = 0$ and has a width in the order of the inverse

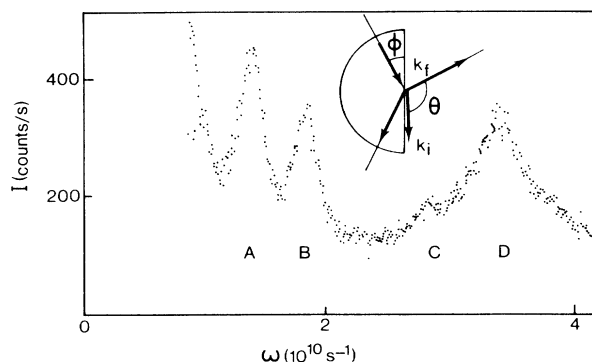


FIG. 1. Typical spectrum from a quartz-propanol interface, with $\theta = 120^\circ$. In the inset we show the scattering geometry. C is scattering from the interface mode, D is the bulk propanol Brillouin peak, A and B are quartz Brillouin peaks: A direct, order 2; B totally reflected, order -2 (the order is the multiple of FSR to be added to ω). The high intensity at zero frequency (5×10^6 counts/s) is due to interface imperfections. The full frequency scale equals half of the free spectral range.

effective penetration depth $1/\xi_{\text{eff}} = 1/\xi_{\text{hyd}} + 1/\xi_{\text{opt}}$, where ξ_{hyd} and ξ_{opt} are the hydrodynamical and optical penetration lengths of the interface mode and the evanescent wave, respectively. Thus the scattering vector in a scattering experiment does not necessarily have to lie along the interface. In the limit $1/\xi_{\text{opt}}^2 \ll k^2$, which pertains to our experimental situation, the absolute value and the tangential component of \mathbf{k} are related to θ as $k = 2k_f \sin(\frac{1}{2}\theta)$ and $k_{\parallel} = 2k_f \sin^2(\frac{1}{2}\theta)$, with $k_f = 2\pi n/\lambda$ where n is the index of refraction of the liquid.

Interface roughness contributes to an intense Rayleigh peak at $\omega = 0$. The contrast of the triple-pass Fabry-Perot interferometer is enough to suppress the wings of this peak in the vicinity of the Brillouin peaks. A complication is scattering from the incident and totally reflected beams by bulk phonons in the quartz itself; the resulting Brillouin peaks add up to the measured spectra. Because the (longitudinal) sound velocity is much larger in quartz than in common liquids, for which the free spectral range has been optimized, these peaks are observed as "higher-order" peaks: they have a frequency outside the interval $\{-\frac{1}{2}\nu_{\text{FSR}}, \frac{1}{2}\nu_{\text{FSR}}\}$ but are mapped onto this interval by subtraction of an integer multiple of FSR. The scattering angles θ must be carefully chosen to keep these peaks away from the (θ -dependent) frequency region of interest for the fluid interface modes.

RESULTS AND DISCUSSION

As liquids we used propanol ($c = 1210$ m/s), ethanol ($c = 1180$ m/s), and a 50 wt. % mixture of methanol and glycerine ($c = 1400$ m/s). A typical spectrum obtained at a propanol-quartz interface is shown in Fig. 1. The low-frequency side is dominated by the intense Rayleigh peak at $\omega = 0$ and the two Brillouin peaks from scattering inside the quartz. The remaining two peaks are the bulk Brillouin peak of the liquid and, on its low-frequency side, a weak peak which we have identified as scattering from the fluid interface mode. For comparison of bulk and interface scattering, the sample was turned through 0.5° to create a homogeneous plane wave in the liquid with approximately the same scattering vector as in the evanescent wave geometry. Then the interface peak disappeared and the bulk Brillouin peak gained one to two orders of magnitude in intensity, without change in either position or width. Figure 2 demonstrates the usual linear ($\omega = ck$) dispersion of the bulk sound mode for propanol. The interface points appear below this line, obviously not on a similar straight line through the origin. For the dispersion relation of these points, only the k_{\parallel} component of the wave vector is predicted to be relevant, with a linear relation $\omega = c_i k_{\parallel}$ in the region $(k_{\parallel} \nu c)^{1/2} \rho / \rho_s (c/c_t)^2 \ll 1$ (Ref. 2) and a slope $c_i = c$ in the regime $(\rho/\rho_s)^2 (c/c_t)^4 \ll 1$ (Ref. 3) (ν is the kinematic viscosity of the liquid). Both conditions are satisfied in our case. Therefore, we plotted the interface points against k_{\parallel} instead of k (Fig. 3). It appears that the points below $k_{\parallel} = 2.5 \times 10^7 \text{ m}^{-1}$ are approximately on the predicted line $\omega = ck_{\parallel}$. The remaining propanol point and the two ethanol points can be matched to the dispersion relation

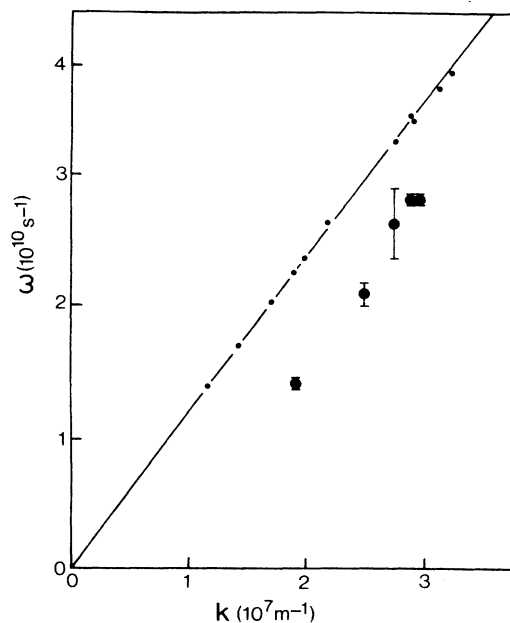


FIG. 2. Dispersion relation ω vs k of propanol. Small dots; bulk. Large dots: interface propanol quartz. The straight line has a slope equal to the bulk sound velocity $c = 1210$ m/s.

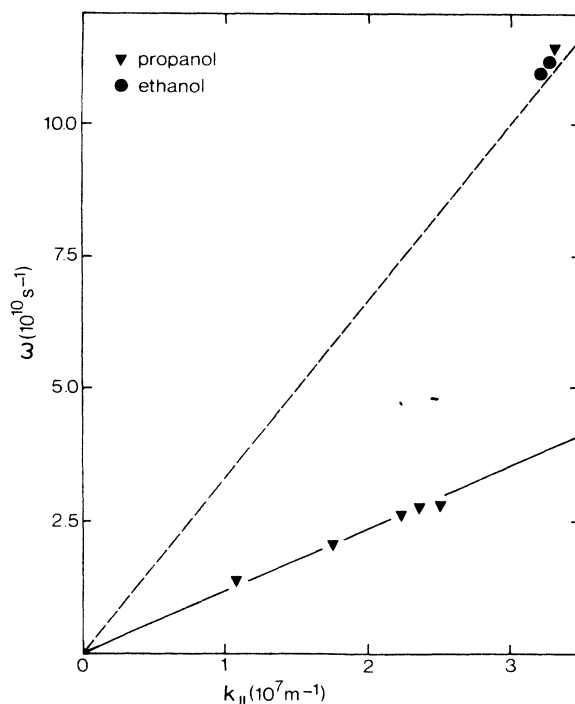


FIG. 3. Dispersion relation ω vs k_{\parallel} of propanol/quartz (triangles) and ethanol/quartz (circles) interface modes. Solid line: fluid interface mode, $\omega = ck_{\parallel}$, $c = 1210$ m/s. Dashed line: Rayleigh wave (from first-order spectrum with $\text{FSR} = 2.68 \times 10^{10} \text{ s}^{-1}$), $\omega = c_R k_{\parallel}$, $c_R = 3340$ m/s.

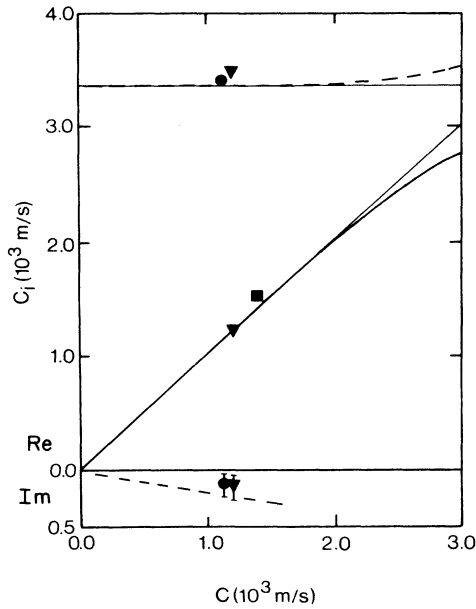


FIG. 4. Sound velocity of quartz-liquid interface modes vs liquid bulk sound velocity (▲, propanol; ●, ethanol; ■, glycerol-methanol) for $\rho_s = 2.1 \text{ g/cm}^3$ and $\rho = 0.8 \text{ g/cm}^3$ (typical for propanol and ethanol). The lines are calculated for the $k_{\parallel} \rightarrow 0$ limit. Solid line: fluid interface mode. Dashed lines: "Rayleigh" wave (real and imaginary parts).

of Rayleigh waves on the quartz surface: $\omega = c_R k_{\parallel}$ with $c_R = 3340 \text{ m/s}$. The peaks produced by these Rayleigh waves are slightly broadened compared to the bulk quartz peaks. Mode coupling between the Rayleigh waves and the fluid interface waves predicts that the velocities of both these modes are roots c_i of the equation³

$$\frac{\rho/\rho_s}{[1-(c_i/c)^2]^{1/2}} = 4(c_i/c_i)^3[(c_i/c_i)^2-1]^{1/2} + \frac{[2(c_i/c_i)^2-1]^2}{[1-(c_i/c_i)^2]^{1/2}},$$

where c_l is the longitudinal sound velocity in the solid. This equation is correct up to the order k in the dispersion relation; it does not account for dissipative effects which are of higher order (k^2 in bulk, $k_{\parallel}^{3/2}$ at interfaces^{1,2}). Parameters for quartz are $\rho_s = 2.1 \text{ g/cm}^3$, $c_l = 5730 \text{ m/s}$, $c_t = 3720 \text{ m/s}$; c_R is one of the roots for $\rho = 0$. In Fig. 4 the measured velocities at the interface are compared with the mode-coupling equation. The damping $\text{Im}(c_i)$ of the Rayleigh waves is due to the excitation of bulk phonons in the liquid to which they lose energy. Such a process is possible without violating the conservation of k_{\parallel} and because $c_R > c$. The Rayleigh waves then belong to the class of leaky waves. Since dissipative damping of sound in quartz is negligible, the observed broadening of the peaks of the Rayleigh waves must be due to this effect. The analogous process, in which the interfacial fluid mode would lose energy into the solid, is not possible because $c_t, c_l > c_i$. Damping is then mainly due to viscous dissipation and the predicted mode-coupling effects (order $k_{\parallel}^{3/2}$) on the peak width are too small to be observed in our case.

To summarize, we observed an interfacial fluid mode at a solid-liquid interface with a dispersion relation $\omega = ck_{\parallel}$, and a damped Rayleigh mode whose width is consistent with mode-coupling theory. Experiments are in progress for cases with $c \approx c_R$, where stronger mode coupling is anticipated.

ACKNOWLEDGMENTS

This work is part of the scientific program of the Foundation for Fundamental Research on Matter (FOM) with financial support from the Netherlands Organisation for Research (NWO), under Project No. 86-542.

¹D. Gutkowitz-Krusin and I. Procaccia, Phys. Rev. Lett. **48**, 417 (1982); Phys. Rev. A **27**, 2585 (1983).

²D. Gutkowitz-Krusin, Phys. Rev. A **28** 2802 (1983).

³L. M. Brekhovskikh, *Waves in Layered Media* (Academic, New York, 1980).

⁴J. G. Dil and N. C. J. van Hijningen, Phys. Rev. B **22**, 5924

(1980).

⁵J. G. Dil, Rep. Prog. Phys. **45**, 285 (1982).

⁶R. Loudon and J. R. Sanderock, J. Phys. C **13**, 2609 (1980).

⁷B. Berne and R. Pecora, *Dynamic Light Scattering* (Wiley, New York, 1976).